Astronomy & Astrophysics

L<small>ETTER TO THE</small> E<small>DITOR</small>

Constraining planet structure from stellar chemistry: the cases of CoRoT-7, Kepler-10, and Kepler-93[⋆,⋆⋆]

N. C. Santos[1,2], V. Adibekyan[1], C. Mordasini[3], W. Benz[3], E. Delgado-Mena[1], C. Dorn[3], L. Buchhave[4,5], P. Figueira[1], A. Mortier[6], F. Pepe[7], A. Santerne[1], S. G. Sousa[1], and S. Udry[7]

[1] Instituto de Astrofísica e Ciências do Espaço, Universidade do Porto, CAUP, Rua das Estrelas, 4150-762 Porto, Portugal
e-mail: nuno@astro.up.pt
[2] Departamento de Física e Astronomia, Faculdade de Ciências, Universidade do Porto, Rua Campo Alegre, 4169-007 Porto, Portugal
[3] Physikalisches Institut, University of Bern, Sidlerstrasse 5, 3012, Bern, Switzerland
[4] Harvard-Smithsonian Center for Astrophysics, Cambridge, Massachusetts 02138, USA
[5] Centre for Star and Planet Formation, Natural History Museum of Denmark, Univ. of Copenhagen, 1350 Copenhagen, Denmark
[6] SUPA, School of Physics and Astronomy, University of St Andrews, St Andrews KY16 9SS, UK
[7] Observatoire de Genève, Université de Genève, 51 ch. des Maillettes, 1290 Sauverny, Switzerland

ABSTRACT

Aims. We explore the possibility that the stellar relative abundances of different species can be used to constrain the bulk abundances of known transiting rocky planets.
Methods. We use high resolution spectra to derive stellar parameters and chemical abundances for Fe, Si, Mg, O, and C in three stars hosting low mass, rocky planets: CoRoT-7, Kepler-10, and Kepler-93. These planets follow the same line along the mass-radius diagram, pointing toward a similar composition. The derived abundance ratios are compared with the solar values. With a simple stoichiometric model, we estimate the iron mass fraction in each planet, assuming stellar composition.
Results. We show that in all cases, the iron mass fraction inferred from the mass-radius relationship seems to be in good agreement with the iron abundance derived from the host star's photospheric composition.
Conclusions. The results suggest that stellar abundances can be used to add constraints on the composition of orbiting rocky planets.

Key words. planetary systems – planets and satellites: detection – stars: abundances – techniques: spectroscopic

1. Introduction

The study of chemical abundances in stars with planetary companions proved to be fundamental for our understanding of the formation of planetary systems as a whole (Ida & Lin 2004; Mordasini et al. 2012). Important clues for the processes of planet formation and evolution have been brought by the discovery that the frequency of giant planets is a strong function of stellar metallicity (e.g. Santos et al. 2004; Fischer & Valenti 2005), as well as by the fact that such a correlation does not seem to be present for stars hosting lower mass planets (Sousa et al. 2011; Buchhave et al. 2012) – see, however, discussions in Adibekyan et al. (2012a) and Wang & Fischer (2015). Also, the stellar chemical composition seems to be related to the structure of the planets that were formed: the heavy element content of a giant planet seems to correlate with the host star metallicity (Guillot et al. 2006; Fortney et al. 2007). The whole planetary architecture (e.g., orbital periods and eccentricities) may be related to the presence of heavy elements in the stellar host (Beaugé & Nesvorný 2013; Dawson & Murray-Clay 2013; Adibekyan et al. 2013).

Specific relative abundances of chemical species may also be reflected in the bulk composition of the planets (e.g., Grasset et al. 2009). Different chemical abundances in the disk may

result in the formation of planets that have different composition and structure (Carter-Bond et al. 2012), something that may even change their habitability potential (Noack et al. 2014). Understanding whether the relative chemical abundances we measure in the photosphere of the host star are related to the relative bulk composition of its orbiting planet(s) may thus provide valuable clues for modeling planet structure once precise masses and radii are measured.

Recently, Dressing et al. (2015) has shown that five known rocky planets (Kepler-10b, Kepler-36b, Kepler-78b, Kepler-93b, and CoRoT-7b) with precise measurements of the mass (relative uncertainties less than 20%) and radius all seem to fall along the same line in the mass-radius diagram: the area corresponding to an approximately Earth-like composition with a silicate mantle and an iron core of a similar mass fraction. Their best fit-model is comprised of 17% iron and 83% silicate mantle ($MgSiO_3$), using a simple two-component interior structure model (Zeng & Sasselov 2013). This is within 20% of the iron mass fractions estimates of Earth, Venus, and Mars with 36%, 30−36%, and 23−25% derived, respectively (Reynolds & Summers 1969), using a comparable model that assumes no iron oxides in the mantle. More detailed studies strongly suggest that relative abundances of Fe, Mg, and Si are similar among the Sun, Earth, Mars, Venus, as well as meteorites (e.g., Lodders 2003; Drake & Righter 2002; Lodders & Fegley 1998; Khan & Connolly 2008; Sanloup et al. 1999). Meteorites are believed to be chemically similar to the building blocks of planets (Morgan & Anders 1980), because both are condensates from the solar nebula that experienced the same fractionation processes. In the solar system the Sun's photospheric relative Fe-abundance can

---

thus be used as a proxy for the iron mass fraction for three out of four terrestrial planets. This fraction is in turn a key quantity for the characterization of exoplanets: from measurement of mass and radius alone, the interior composition can only be weakly constrained owing to model degeneracies (Dorn et al. 2015).

It is thus interesting to see whether for the planets analyzed by Dressing et al. (2015), a compositional correlation between the host stars and their planets is possible, suggesting that it may not be restricted to the solar system case. This is predicted by planet formation models that include equilibrium condensation models corresponding to small distances to the host star (~1 AU). As a consequence, these relative abundances do not vary significantly within a disk, whether spatially and temporally (e.g., Johnson et al. 2012; Thiabaud et al. 2014)[1]. If we find observational evidence that many exoplanets follow a mass-radius relation that agrees with the relative composition in refractories of their host stars, this would mean that we can use stellar composition as a proxy to reduce the degeneracy of possible interior models, more specifically, by coupling structure and composition of core and mantle through bulk abundance ratios (e.g. Dorn et al. 2015).

With the goal of testing these possibilities, we present a detailed study of the chemical abundances for three out of five of the planets discussed in Dressing et al. (2015): Kepler-10b, Kepler-93b, and CoRoT-7b. In Sects. 2 and 3 we present our data, the derivation of stellar parameters, and chemical abundances. We then discuss the results in Sect. 4.

2. Observations and data

Spectra for Kepler-10 and Kepler-93 were obtained from the SOPHIE archive (OHP 1.93-m telescope). The data was gathered as part of a program to derive masses and confirm the planetary nature of detected *Kepler* candidates (e.g., Santerne et al. 2012). The spectra cover the range between 3870 and 6940 Å. The spectra were obtained using the high resolution mode (HR; $R = 75\,000$) for Kepler-10, and the high efficiency mode (HE; $R = 40\,000$) for Kepler-93. In both cases Fiber B of the spectrograph was pointed toward a sky region. The spectra were reduced using the SOPHIE pipeline. The sky spectra were subtracted from the stellar spectrum using the information available in Fiber B after correcting for the efficiency difference between the two fibers. For Kepler-10 we combined five spectra obtained between 2011 July 7 and 2011 September 9 (other available spectra had very poor S/N). For Kepler-93 we combined two spectra obtained on the nights of 2014 March 13 and 2014 April 26. The S/N of the final spectra is in the range of 80 and 60 as measured using continuum regions near 6500 Å, respectively.

For Kepler-10 we also gathered spectra obtained using the high resolution ($R = 115\,000$) HARPS-N spectrograph (Cosentino et al. 2012) – courtesy of the HARPS-N consortium. We combined a total of 110 high S/N spectra ($S/N > 50$ in order 50) obtained between 2012 May 25 and 2013 October 18. The final spectrum has a S/N on the order of 600. A comparison between the results obtained using the SOPHIE and HARPS-N spectra gives us an idea about the possible systematic errors between parameters and abundances derived using different spectra.

As we see below, we have already analyzed an existing HARPS spectrum for CoRoT-7. We point the reader to Mortier et al. (2013) for further details.

---

[1] For a specific planet it is possible that an external process may have significantly altered its bulk composition like was the case for Mercury.

3. Stellar parameters and abundances

Stellar parameters for Kepler-10 (independently derived from the SOPHIE and HARPS-N spectra) and Kepler-93 were derived in LTE, using a grid of plane-parallel, ATLAS9 model atmospheres (Kurucz 1993) and the radiative transfer code MOOG (Sneden 1973). The methodology used is described in detail in Sousa et al. (2011). The full spectroscopic analysis is based on the equivalent widths (EWs) of ~250 Fe I and 40 Fe II weak lines by imposing ionization and excitation equilibrium. Parameters for CoRoT-7 have already been derived by our team (using the same tools and methods) from a high resolution, high S/N HARPS spectrum (Mortier et al. 2013).

For FGK dwarfs the effective temperatures obtained using this methodology were shown to be compatible with estimates from recent applications of the infrared flux method (see, e.g., Santos et al. 2013). Possible errors in the derived (always more uncertain) $\log g$ have little or no influence on the abundances of individual species as derived from atomic (non-ionized) lines.

The derived parameters for the three stars are listed in Table A.1, where we also list literature values for comparison. It is interesting that the parameters and abundances derived for Kepler-10 using the two spectra are similar despite the lower S/N and resolution of the SOPHIE data.

3.1. Chemical abundances: Si, Mg, C, and O

The abundances of magnesium (Mg) and silicon (Si) were derived for the three stars following the same methodology as in our previous works (e.g., Adibekyan et al. 2012a, 2015). We used a LTE analysis relative to the Sun with the 2014 version of the code MOOG (Sneden 1973) and a grid of Kurucz ATLAS9 plane-parallel model atmospheres with no α-enhancement. For the EW measurements, we used ARES2 (Sousa et al. 2015), for which the input parameters were the same as in Sousa et al. (2011). A visual inspection was done to confirm the reliability of the ARES2 measurements.

The abundances for each star and element were calculated from the average of the values provided by all measured lines (3 lines for Mg and 16 lines for Si). A two-sigma clipping cut was performed to remove outliers. Errors in the abundances of the elements [X/H] were evaluated adding quadratically the line-to-line scatter errors and errors induced by uncertainties in the model atmosphere parameters (see, e.g., Adibekyan et al. 2012a). The final abundances of Mg and Si are presented in Table A.1. For CoRoT-7, abundances for Mg and Si perfectly match the ones derived in Mortier et al. (2013) using an older version of MOOG.

Carbon (C) and oxygen (O) abundances were derived with the same tools as Mg and Si but measuring the EWs of the lines with the task *splot* in IRAF. Atomic data for the O lines and for the Ni line-blend affecting the oxygen forbidden line at 6300 Å were taken from Bertran de Lis et al. (2015). The data for the atomic carbon lines was taken from the VALD3 database[2].

The final abundances derived using each individual line are shown in Table A.2. The errors for the abundances are mainly due to the uncertainties in the position of the continuum. In the error estimate, we also considered the sensitivity of the C and O abundances due to the error in the atmospheric parameters, adding all terms quadratically as done for Mg and Si. The error caused by the continuum placement was estimated by recalculating the abundance using different continuum positions as measured by hand. Unfortunately, the S/N of the SOPHIE spectra is
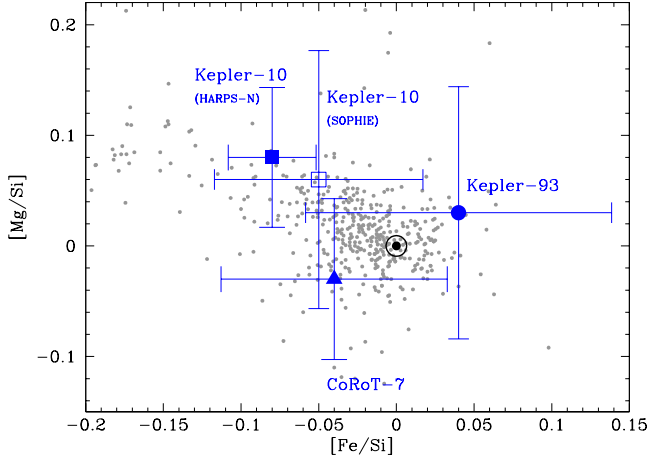
---

[2] http://vald.astro.univie.ac.at/~vald3/php/vald.php

Fig. 1. [Mg/Si] vs. [Fe/Si] for the studied stars, together with the comparison dwarf (gray small dots) from Adibekyan et al. (2012b) with $T_{\mathrm{eff}} = T_{\odot} \pm 300$ K. The position of the Sun is shown for comparison.

not high enough to allow us to measure the weak oxygen lines. Furthermore, the HARPS-N spectra for Kepler-10 shows telluric contamination in the region of the oxygen forbidden line. For CoRoT-7 the oxygen line at 6158 Å is too weak. Therefore we could only derive C/O ratios for Kepler-10 and CoRoT-7, based on a single oxygen indicator each.

For reference, the solar values are also shown Table A.2. While the carbon abundance in the Sun is well defined using the C I atomic lines, the oxygen abundance is more uncertain, and the different indicators (lines) provide different values (see discussion in Bertran de Lis et al. 2015). Therefore, in Table A.2 we give the oxygen abundance values individually. The [C/O] ratio is also computed using the corresponding solar abundance, depending on which oxygen line we could use.

4. Discussion and conclusions

In Fig. 1 we show the position of the stars in the [Mg/Si]−[Fe/Si] plane. The plot shows that while Kepler-93 and CoRoT-7 do not seem to have significantly different abundance ratios than the Sun, the situation for Kepler-10 seems different. Both the abundances derived from the SOPHIE and HARPS-N spectra suggest that the star has a [Fe/Si] below solar (−0.08/−0.05 from HARPS-N and SOPHIE data, respectively). The [Mg/Si] ratio observed in Kepler-10 also seems to be above solar (0.08/0.06 from HARPS-N and SOPHIE data, respectively). In this sense it is interesting to see that both sets of spectra provide very similar results, even if the whole analysis was done in a fully independent way. It is worth noting that since the model changes (variation in stellar parameters) induce similar effects in the abundances of these refractory elements (they partially cancel out when computing the ratios [X1/X2]), our reported errors are likely conservative.

For Kepler-10 we find evidence for abundance ratios that are significantly different from solar, though the differences are not higher than ~0.1 dex. For CoRoT-7 and Kepler-93, on the other hand, the abundance ratios seem to be very similar to solar. Following the galactic chemical evolution trends (Bensby et al. 2005; Adibekyan et al. 2012b), we could expect that stars with [Fe/H] below solar should on average present [Si/Fe] abundances that are slightly above solar (i.e., [Fe/Si] ratios below solar), though perfectly allow the opposite trend given the observed dispersions.

Concerning C and O, we first note that the carbon abundances for Kepler-10, as derived from different spectra (HARPS-N and SOPHIE), agree well within the errors. The [C/O] ratio for this star seems to be subsolar. This is expected since oxygen, as a pure α-element, grows more rapidly than carbon as a function of [Fe/H], for [Fe/H] < 0 (e.g., Bertran de Lis et al. 2015; Bensby et al. 2005). In any case, the observed [C/O] ratio values are not expected to have a significant impact on the bulk composition of the planet (Bond et al. 2010; Delgado Mena et al. 2010) when compared to a solar ratio.

On the other hand, for CoRoT-7 we could expect a [C/O] ratio that is more similar to the solar value owing to its more similar metallicity. However, its elevated oxygen abundance yields a lower [C/O] ratio. Although the determination of oxygen abundances can often be problematic for cooler stars such as CoRoT-7, in this case the quality of the spectrum allowed us to measure the EW of the forbidden line perfectly, and the spectrum does not seem to show telluric contamination in the region (which could produce an artificial enhanced oxygen abundance). We note that the high error of [C/O] for this star precludes firm conclusions.

Whether the observed compositional differences are relevant when modeling the interior structure of the exoplanets is the next obvious question to answer. In particular, we want to know whether the interiors structure of the planets presented by Dressing et al. (2015) can be explained when using the specific stellar abundances as proxies for the planet bulk compositions. Given the large uncertainties on mass and radius, as well as on the abundances, we suppose that (1) this is likely the case and (2) the single model of an Earth-like iron-core mass fraction as used by Dressing et al. (2015) lies within the generally wide range of possible interior models. A detailed analysis of this including a full error analysis will be presented in future theoretical work. Here we only make first simple considerations regarding the relative expected abundances of the most important rock-forming elements and, in particular, of iron.

We only have abundances of Fe, Si, Mg, O, and C. However, these rocky-forming elements, together with H and He, are the most relevant ones for controlling the species expected from equilibrium condensation models, (Lodders 2003; Seager et al. 2007), namely H_2, He, CH_4, H_2O, Fe, $MgSiO_3$, and Mg_2SiO_4 (all stars have $N_{\mathrm{Mg}} > N_{\mathrm{Si}}$). A simplified model for the expected mass fractions of different compounds using these species is thus a reasonable approach. In this chemical network, the molecular abundances and therefore the mass fraction can be found from the atomic abundances with simple stoichometry:

$$N_{\mathrm{O}} = N_{\mathrm{H_2O}} + 3N_{\mathrm{MgSiO_3}} + 4N_{\mathrm{Mg_2SiO_4}} \qquad (1)$$

$$N_{\mathrm{Mg}} = N_{\mathrm{MgSiO_3}} + 2N_{\mathrm{Mg_2SiO_4}} \qquad (2)$$

$$N_{\mathrm{Si}} = N_{\mathrm{MgSiO_3}} + N_{\mathrm{Mg_2SiO_4}}. \qquad (3)$$

Similar equations hold for the other species. This way we calculated the expected mass fractions, in particular f_{iron}, for the three stars analyzed in this paper. Table 1 shows the result in terms of mass fractions m_{X} of the five heavy element species (in percentage points), the total mass fraction of heavy elements Z, and finally the iron mass fraction among the refractory elements, which is the key result. In the table we also showed, for comparison, the results with our basic chemistry model for the Sun using the solar composition of Asplund et al. (2009). The table also contains the condensate abundances derived by Lodders (2003, her Table 11, photospheric values) with a full condensation model that includes a much higher number of species. Kepler-93 (K-93) has no oxygen measurement. We assumed a

Table 1. Mass fractions of heavy element, total fraction of heavy elements, and iron mass fraction among refractory species (values in %).

Quantity	C-7	K-93	K-10	Sun	Sun[f]
H_2O[a]	0.75 ± 0.31	0.54 ± 0.22	0.98 ± 0.20	0.50	0.51
CH_4[a]	0.32 ± 0.05	0.35 ± 0.13	0.36 ± 0.04	0.37	0.29
Fe[a]	0.14 ± 0.01	0.09 ± 0.01	0.10 ± 0.00	0.13	0.17[d]
$MgSiO_3$[a]	0.25 ± 0.08	0.10 ± 0.06	0.11 ± 0.05	0.19	0.27[e]
Mg_2SiO_4[a]	0.05 ± 0.06	0.08 ± 0.06	0.14 ± 0.06	0.08	
Z[b]	1.50 ± 0.31	1.17 ± 0.25	1.69 ± 0.21	1.26	1.32
$f_{\rm iron}$[c]	31.6 ± 2.6	34.7 ± 3.7	27.5 ± 1.7	33.2	38.0

Notes. [a] The m_{H2} and m_{He} are between 74.7−75.1% and 23.6−23.7%, respectively. [b] Summed mass percent of all heavy elements. [c] $m_{Fe}/(m_{Fe} + m_{MgSiO3} + m_{Mg2SiO4})$. [d] Includes all metal species and FeS. [e] Includes all silicates and oxides. [f] Lodders (2003).

solar oxygen abundance for this star. This is a good assumption given the expected oxygen-to-iron ratio for stars with such metallicity (e.g., Bertran de Lis et al. 2015). Error bars were derived as explained in Appendix B.

The table shows that owing to the approximately scaled solar composition of CoRoT-7 (C-7) and Kepler-93 (under the assumption of solar N_O), their $f_{\rm iron}$ is very similar to the one of the Sun (32−35%). Only for Kepler-10 (K-10), which is more depleted in Fe than in Mg and Si relative to the Sun, do we see a slightly lower $f_{\rm iron}$ = 27.5% (and higher H_2O), as expected. Curiously, both Kepler-10b and Kepler-10c seem to be "oversized" in the mass-radius diagram of Dressing et al. (2015) when compared to the Earth composition model. In any case, we find that for the three planets analyzed by Dressing et al. (2015), the iron mass fraction inferred from the mass-radius relationship (∼17%) is on a ∼10−20% level, in agreement with the iron abundance derived here from the host star photospheric composition, and in even better agreement with the mass fraction (∼29−32%) expected from more detailed models of solar system planets (for the Earth see, e.g., McDounough & Sun 1995). If confirmed, this interesting result doubles the number of rocky planets (including the solar system's) where the mass of the iron core can be estimated if the stellar composition is known, and brings it to six out of seven rocky planets where such an inference can be made (the exception is Mercury). As discussed in the introduction, this is important for reducing the compositional degeneracy of planet interiors (Dorn et al. 2015) and for constraining impact events.

A much more detailed analysis that combines host star abundances, mass and radius measurements, and internal structure calculations should be done in future work, taking all the associated measurement and model uncertainties into account. If the agreement of the planetary core mass (derived from the $M − R$ relationship) and the stellar photospheric abundances found here is confirmed and extended to additional planets, this would allow a better characterization of exoplanet interiors, even if a significantly different composition (as for Mercury) cannot be excluded a priori for an individual planet. This shows that a detailed chemical analysis of exoplanet hosts is important not only for the architecture of a planetary system, but also for the interior structure, composition, and potential habitability of individual planets. The detailed characterization of planets discovered and characterized by future space missions such as TESS, CHEOPS, and PLATO-2.0 will certainly gain from this analysis.

References

Adibekyan, V. Z., Delgado Mena, E., Sousa, S. G., et al. 2012a, A&A, 547, A36
Adibekyan, V. Z., Sousa, S. G., Santos, N. C., et al. 2012b, A&A, 545, A32
Adibekyan, V. Z., Figueira, P., Santos, N. C., et al. 2013, A&A, 560, A51
Adibekyan, V. Z., Benamati, L., Santos, N. C., et al. 2015, MNRAS, 450, 1900
Asplund, M., Grevesse, N., Sauval, A. J., & Scott, P. 2009, ARA&A, 47, 481
Ballard, S., Chaplin, W. J., Charbonneau, D., et al. 2014, ApJ, 790, 12
Batalha, N. M., Borucki, W. J., Bryson, S. T., et al. 2011, ApJ, 729, 27
Beaugé, C., & Nesvorný, D. 2013, ApJ, 763, 12
Bensby, T., Feltzing, S., Lundström, I., & Ilyin, I. 2005, A&A, 433, 185
Bertran de Lis, S., Delgado Mena, E., Adibekyan, V. Z., Santos, N. C., & Sousa, S. G. 2015, A&A, 576, A89
Bond, J. C., O'Brien, D. P., & Lauretta, D. S. 2010, ApJ, 715, 1050
Bruntt, H., Deleuil, M., Fridlund, M., et al. 2010, A&A, 519, A51
Buchhave, L. A., Latham, D. W., Johansen, A., et al. 2012, Nature, 486, 375
Carter-Bond, J. C., O'Brien, D. P., & Raymond, S. N. 2012, ApJ, 760, 44
Cosentino, R., Lovis, C., Pepe, F., et al. 2012, in SPIE Conf. Ser. 8446, 1
Dawson, R. I., & Murray-Clay, R. A. 2013, ApJ, 767, L24
Delgado Mena, E., Israelian, G., González Hernández, J. I., et al. 2010, ApJ, 725, 2349
Dorn, C., Khan, A., Heng, K., et al. 2015, A&A, 577, A83
Drake, M. J., & Righter, K. 2002, Nature, 416, 39
Dressing, C. D., Charbonneau, D., Dumusque, X., et al. 2015, ApJ, 800, 135
Dumusque, X., Bonomo, A. S., Haywood, R. D., et al. 2014, ApJ, 789, 154
Fischer, D. A., & Valenti, J. 2005, ApJ, 622, 1102
Fortney, J. J., Marley, M. S., & Barnes, J. W. 2007, ApJ, 659, 1661
Grasset, O., Schneider, J., & Sotin, C. 2009, ApJ, 693, 722
Guillot, T., Santos, N. C., Pont, F., et al. 2006, A&A, 453, L21
Ida, S., & Lin, D. N. C. 2004, ApJ, 616, 567
Johnson, T. V., Mousis, O., Lunine, J. I., & Madhusudhan, N. 2012, ApJ, 757, 192
Khan, A., & Connolly, J. A. D. 2008, J. Geophys. Res., 113, E07003
Kurucz, R. 1993, CD-ROM No. 13 (Cambridge, Mass.: Smithsonian Astrophysical Observatory)
Léger, A., Rouan, D., Schneider, J., et al. 2009, A&A, 506, 287
Lodders, K. 2003, ApJ, 591, 1220
Lodders, K., & Fegley, B. 1998, The planetary scientist's companion (New York: OUP)
McDounough, W. F., & Sun, S.-s. 1995, Chemical Geology, 120, 223
Mordasini, C., Alibert, Y., Benz, W., Klahr, H., & Henning, T. 2012, A&A, 541, A97
Morgan, J. W., & Anders, E. 1980, PNAS, 77, 6973
Mortier, A., Santos, N. C., Sousa, S. G., et al. 2013, A&A, 558, A106
Noack, L., Godolt, M., von Paris, P., et al. 2014, Planet. Space Sci., 98, 14
Reynolds, R. T., & Summers, A. L. 1969, J. Geophys. Res., 74, 2494
Sanloup, C., Jambon, A., & Gillet, P. 1999, Physics of the Earth and Planetary Interiors, 112, 43
Santerne, A., Díaz, R. F., Moutou, C., et al. 2012, A&A, 545, A76
Santos, N. C., Israelian, G., & Mayor, M. 2004, A&A, 415, 1153
Santos, N. C., Sousa, S. G., Mortier, A., et al. 2013, A&A, 556, A150
Seager, S., Kuchner, M., Hier-Majumder, C. A., & Militzer, B. 2007, ApJ, 669, 1279
Sneden, C. 1973, Ph.D. Thesis, Austin, Univ. of Texas
Sousa, S. G., Santos, N. C., Israelian, G., Mayor, M., & Udry, S. 2011, A&A, 533, A141
Sousa, S. G., Santos, N. C., Adibekyan, V., Delgado-Mena, E., & Israelian, G. 2015, A&A, 577, A67
Thiabaud, A., Marboeuf, U., Alibert, Y., et al. 2014, A&A, 562, A27
Wang, J., & Fischer, D. A. 2015, AJ, 149, 14
Zeng, L., & Sasselov, D. 2013, PASP, 125, 227

Page 5 is available in the electronic edition of the journal at http://www.aanda.org

Appendix A: Stellar parameters and chemical abundances

Table A.1. Stellar atmospheric parameters and iron, magnesium, and silicon abundances for our targets.

Star	T_{eff} (K)	$\log g$ (dex)	ξ (km s^{-1})	[Fe/H] (dex)	[Mg/H] (dex)	[Si/H] (dex)	Source	Instrument
Kepler-10	5671 ± 17	4.34 ± 0.01	0.92 ± 0.02	−0.14 ± 0.02	+0.02 ± 0.06	−0.06 ± 0.02	This paper	HARPS-N
Kepler-10	5614 ± 39	4.27 ± 0.04	0.82 ± 0.05	−0.14 ± 0.03	−0.03 ± 0.10	−0.09 ± 0.06	This paper	SOPHIE
Kepler-93	5689 ± 48	4.56 ± 0.06	1.02 ± 0.07	−0.15 ± 0.04	−0.16 ± 0.07	−0.19 ± 0.09	This paper	SOPHIE
CoRoT-7	5288 ± 27	4.40 ± 0.07	0.90 ± 0.05	+0.02 ± 0.02	+0.03 ± 0.03	+0.07 ± 0.08	Mortier et al. (2013)	HARPS
Literature values:								
Kepler-10	5627 ± 44	4.34 ± 0.01		−0.15 ± 0.04			Batalha et al. (2011)	
	5721 ± 26	4.34		−0.14 ± 0.02			Dumusque et al. (2014)	
Kepler-93	5669 ± 75	4.47 ± 0.01		−0.18 ± 0.10			Ballard et al. (2014)	
CoRoT-7	5250 ± 60	4.47 ± 0.05		+0.12 ± 0.06			Bruntt et al. (2010)	
	5275 ± 75	4.50 ± 0.10		+0.03 ± 0.06			Léger et al. (2009)	

Table A.2. Carbon and oxygen abundances (in dex) for our stars and the Sun, using the Kurucz Solar Atlas (Kurucz et al. 1984).

Star	$\log C_{5052\,Å}$	$\log C_{5380\,Å}$	$\log O_{6158\,Å}$	$\log O_{6300\,Å}$	[C/H]	[O/H]	[C/O]	C/O[e]	Mg/Si[e]
Kepler-10[b]	8.48	8.47	8.92	—	−0.01 ± 0.05	0.21 ± 0.08	−0.22 ± 0.10	0.36	1.48
Kepler-10[a]	8.52	8.44	—	—	0.00 ± 0.08	—	—	—	1.41
Kepler-93[a]	8.35	8.59	—	—	−0.02 ± 0.16	—	—	—	1.32
CoRoT-7[c]	8.38	8.48	—	8.83	−0.06 ± 0.07	0.18 ± 0.15	−0.24 ± 0.17	0.40	1.12
Sun	8.48	8.49	8.71	8.65	0.00	0.00	0.00	0.64[d]	1.23

Notes. [a] SOPHIE. [b] HARPS-N. [c] HARPS. [d] C/O ratios derived using the average values for the oxygen and carbon abundances given by different lines. [e] $A/B = N_A/N_B = 10^{\log \varepsilon(A)}/10^{\log \varepsilon(B)}$, where $\log \varepsilon(A)$ and $\log \varepsilon(B)$ are the absolute abundances.

Appendix B: Errors

The errors in the mass fractions were calculated using a Monte Carlo approach. We randomly drew 10^5 values of the derived stellar abundances abundances following a Gaussian distribution centered on the derived abundance and with a sigma corresponding to the derived errors as listed in Tables A.1 and A.2. For each drawn set of [Si/H], [Mg/H], [O/H], and [C/H], we then computed the expected fractions. The distribution of the resulting values allowed us to derive the one-sigma error, as listed in Table 1.

We note that this procedure was done in a self consistent way. All the mass fractions were computed simultaneously for each set of input abundances. This is important because the resulting mass fraction values are correlated between themselves.

For Kepler-93, since the oxygen abundance was assumed to be solar (no O abundance could be derived from our data), we considered that the [O/H] has an uncertainty of 0.15 dex.